Indian J. Phys. **73A** (2), 133–146 (1999)

IJP A
— an international journal

Magnetic field dependence of critical current density of ceramic HTSCs

D Roy* and A Nag

Department of Physics, University of Kalyani, Kalyani-741 235, West Bengal, India

*Present address : Energy Research Unit, Indian Association for the Cultivation of Science, Jadavpur, Calcutta-700 032, India

Received 23 December 1997, accepted 26 May 1998

Abstract : Magnetic field dependence of transport critical current density $< j_c >$ of Dy 123 HTSC (High Temperature Superconductor)s in low fields (< 150 G) is shown to be satisfactorily accounted for in the frame work of critical state model assuming the generalised power law behaviour $j_c(H) = j_{Co}(1 + |H(x)|/H_0)^{-\beta}$ with $\beta = 1.5$ Experimental $< j_c > (H)/< j_c > (0)$ is also very well reproduced by values calculated from hysteresis magnetisation loop obtained using the same model

Keywords : HTSC, transport critical currents, hysteresis magnetisation

PACS Nos. : 75.60 Ej, 74.60.Jg

1. Introduction

Our object in this paper is to try to connect in case of ceramic granular HTSCs the average critical current density $< j_c >$ at a particular external applied magnetic field H_a, a global quantity, to local critical current density $j_c(H)$ which is a function of the local average field H. $j_c(H)$ is the intergranular current density which again depends on the nature and extent of the intergranular links at the grain boundaries and the microscopic mechanism responsible for superconductivity.

In order to find such a connection, we carefully measured critical current density as a function of applied field H_a on samples in the form of long slabs. From an examination of the general characteristics of such dependence the choice of the functional form of $j_c(H)$ could be narrowed down to the generalised and the modified power law models discussed in Section 3. Calculations of $< j_c > (H_a)$ both from an analysis of transport current in the presence of magnetic field and from hysteresis magnetisation cycle in the frame work of critical state model using generalised relation gave an extremely satisfactory description

© 1999 IACS

of $< j_c > (H_a)$ in the low field region upto nearly 150 G. This work is described in the subsequent sections.

2. Measurement of critical current density

Samples were made by the standard solid state reaction method and were found to be single phase by XRD. These were characterised by routine resistivity and susceptibility measurements. Slabs 2 mm × 2 mm × 15 mm were used. In the four terminal arrangement, voltage drop across voltage terminals (3 mm spacing) was monitored by a Solartron 7071 Computing Voltmeter. The current was provided by constant current sources, HP 6186C upto 100 mA and Aplab CCCV source upto 6A. The sample with contacts was directly immersed in liquid N_2 to ensure good thermal contact. The three different samples used in these measurements were pelletised under different pressure but were of the same composition ($DyBa_2Cu_3O_{7-\delta}$).

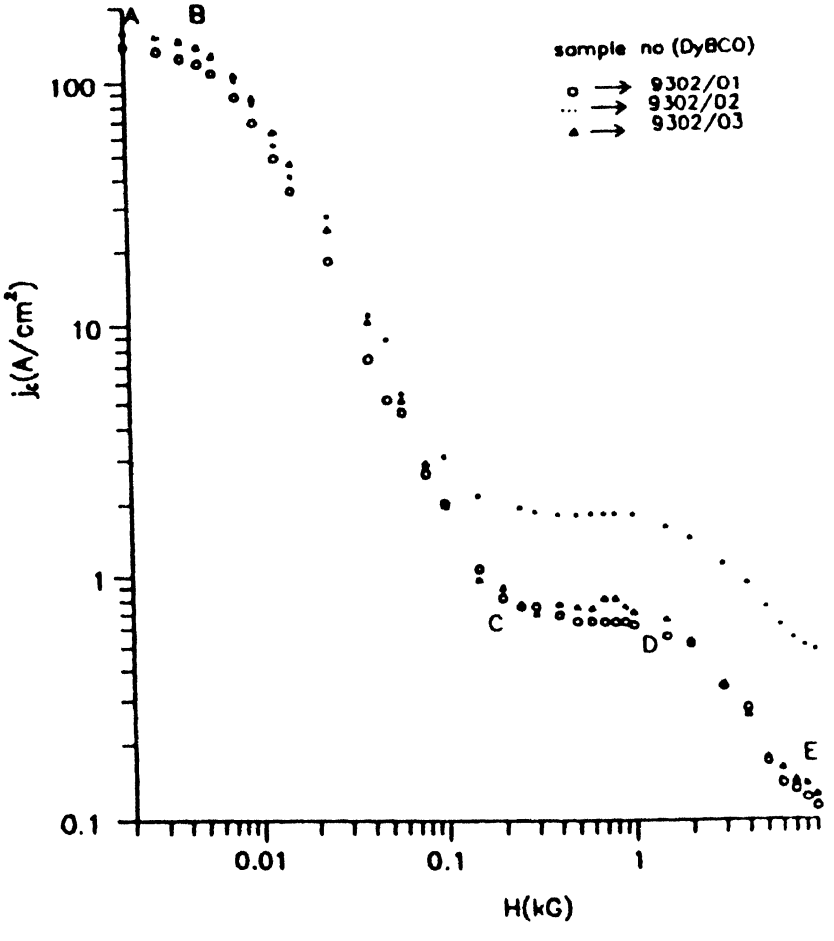

Figure 1. Critical current density $< j_c >$ *vs* H for the three samples. The linear part ($\overline{BC}$) in this log-log plot suggests $< j_c > \propto H^{-\beta}$. The best fit value of $\beta \approx 1.50$.

For the same sample, critical current density was measured in various magnetic fields for transverse, longitudinal, field cooled (FC) and zero field cooled (ZFC) conditions. For very low fields, Helmholtz coil was used. Transport critical current density $< j_c >$ obtained from *V-I* characteristics with 1 μV voltage criterion are shown in Figure 1 against applied magnetic field H_a. The general characteristics are a steep decrease at low fields (part BC) followed by a levelling off for high fields (CD, $H > 100$ Oe) and then again decreasing (for $H > 1$ to 2 kOe). The straight line steep decrease in the log-log plot (part BC) clearly shows that in this region *there is a power law variation* namely $< j_c > \propto (H_a)^{-\beta}$. The fit gives $\beta \simeq 1.5$, 1.46 and 1.54 for samples 1, 2 and 3 respectively. Thus β is nearly 1.50.

3. $< j_c >$ from critical state model

The macroscopic $< j_c >$ in presence of magnetic field can be calculated with the help of critical state model due to Bean [1]. According to Bean's model with a transport current of

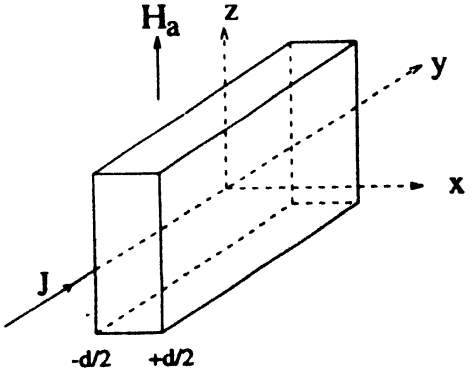

Figure 2. Transport current j flows || to y, H_a is applied || to z. d is the width of the slab along x.

$< j_c >$ along the y direction and H_a along z direction (Figure 2), the local field is obtained from the relation

$$-\frac{4\pi}{10} j_c(H(x)), \tag{1}$$

here j_c is in amp/cm^2 and $H(x)$ is in gauss. The transport current will produce a self-field of magnitude

$$H_s = \frac{4\pi}{10} < j_c > \frac{d}{2}. \tag{2}$$

With H_a applied externally, the boundary conditions are

$$H\left(-\frac{d}{2}\right) = H_2 = H_a + H_s \tag{3a}$$

and

$$H\left(+\frac{d}{2}\right) = H_1 = H_a - H_s. \tag{3b}$$

The field profile has to be obtained by solving eq. (1) with either of the boundary conditions 3(a) or 3(b).

Since $H_2 - H_1 = 2H_s$,

solving it self-consistently gives $< j_c >$ for a given applied field H_a.

The effect of size and magnetic field on critical current density of HTSC has been investigated by many authors [4–10] in the frame work of Ginzburg Landau theory and critical state model [1–3]. In the original Bean model, j_c was taken to be independent of the local field H. The original Bean model was first modified by Anderson and Kim [3]. The Kim model [3] has been used by Ravi Kumar and Chaddah [11], the power law model by Yeshurun *et al* [12] and the exponential model by Ravi Kumar [10] and others [7,8,13,14]. Recently, it has been pointed out that all these critical state models are related and follow from a generalised model [15]

$$j_c(H,T) = \frac{j_c(0,T)}{\left[1 + \dfrac{|H(x)|}{H_0}\right]^{\beta}}. \tag{4}$$

The relation (4) reduces to

(i) Bean model for $\beta = 0$,

(ii) Kim model for $\beta = 1$,

(iii) Power law model for $|H(x)|/H_0 >> 1$,

(iv) Exponential model for $|H(x)|/H_0 << 1$.

A second power law model

$$j_c(H,T) = \frac{j_c(0,T)}{1 + \left(\dfrac{|H(x)|}{H_0}\right)^{\beta}} \tag{5}$$

has been used by Müller *et al* [16] with considerable success.

We shall first try to find out which of these relations for $j_c(H)$ is better suited to account for the field variation of $< j_c >$ in the part AC (Figure 1). In this discussion, $H(x)$ is the average local field and $j_c(H(x))$ is also an average local critical current density, averaged over a large number of grains. We shall make some observations which we shall justify later from detailed calculation. As the field H_a is increased and $< j_c >$ decreases, the effect of self-field will decrease. Therefore, $H(x)$ will become more uniform and so also $j_c(H(x))$. Thus, $< j_c >_{H_a}$ will be more and more equal to $j_c(H)$. We shall also find that the parameter H_0 is of the order of 1 gauss. Since in the region of steep descent (~10 to 100 G), $< j_c > \propto (H_a)^{-\beta}$, so $j_c(H)$ should have similar power law variation with H in this region

$$j_c(H) \approx J_0\left(\frac{|H(x)|}{H_0}\right)^{-\beta} \quad \text{for} \quad \frac{|H(x)|}{H_0} \gg 1.$$

Since β has been found experimentally to be near 1.50, Bean model $\beta = 0$ and Kim model $\beta = 1$ may be ruled out so also the exponential model. The power law model $j_c(H, T) = j_c(0, T)\,(|H(x)|/H_0)^{-\beta}$ suffers from infinity at $H(x) = 0$. Therefore, we shall consider

only the generalised power law model (GPL) (eq. 4) and the modified power law model (MPL) (eq. 5). We shall derive relations using (GPL) and use the relations for $< j_c >$ from (MPL) as obtained by Müller *et al* [7,8].

Thus

$$dH(x)\left[1 + \frac{|H(x)|}{H_0}\right]^{\beta} = -J_0 dx \tag{6}$$

where $J_0 = \frac{4\pi}{10} j_c(0, T)$ subject to boundary conditions (2), 3(a) and 3(b).

As H_a is increased from zero upwards, there are three possible situations for H_1, namely $H_1 < 0$, $H_1 = 0$, $H_1 > 0$.

For $H_1 > 0$, $H(x) > 0$, since $H(d/2) = H_1$,

$$H(x) = \left[(H_0 + H_1)^{\beta+1} + J_0 H_0^{\beta}(\beta+1)(d/2 - x)\right]^{\frac{1}{\beta+1}} - H_0 \tag{7}$$

and

$$\frac{4\pi}{10} < j_c > = \frac{2}{d}\left[J_0 H_0^{\beta} d(\beta+1) + \left(H_0 + H_a - \frac{4\pi}{10} < j_c > d/2\right)^{\beta+1}\right]^{\frac{1}{\beta+1}} - \frac{2}{d}(H_0 + H_a). \tag{8}$$

For $H_1 > 0$ we solve eq. (8) self-consistently to find $< j_c >$, use this value to obtain H_s and then H_1 and applying this value of H_1 in eq. (7) find $H(x)$ and hence $j_c(H(x))$.

For $H_1 < 0$, we have two cases,

case (i) : $H(x) = -\text{ve}$ for $x_1 < x < d/2$;

case (ii) : $H(x) = +\text{ve}$ for $-d/2 < x < x_1$.

case (i) : $|H(x)| = -H(x)$ and $H(d/2) = H_1$,

$$H(x) = H_0 - \left[(H_0 - H_1)^{\beta+1} - J_0 H_0^{\beta}(\beta+1)(d/2 - x)\right]^{\frac{1}{\beta+1}}. \tag{9}$$

With $H(x_1) = 0$,

$$x_1 = \frac{d}{2} - \frac{H_0}{J_0(\beta+1)}\left|1 - \frac{H_1}{H_0}\right|^{\beta+1} - 1\Big|. \tag{10}$$

case (ii) : $|H(x)| = H(x)$ and $H(-d/2) = H_2$,

$$H(x) = \left[(H_0 + H_2)^{\beta+1} - J_0 H_0^{\beta}(\beta+1)(d/2 + x)\right]^{\frac{1}{\beta+1}} - H_0. \tag{11}$$

Using the condition $H(x_1) = 0$ and substituting the value of x_1 from eq. (10)

$$\frac{4\pi}{10} < j_c > = \frac{2}{d}\left[2H_0^{\beta+1} + J_0 H_0^{\beta} d(\beta+1) - \left(H_0 - H_a + \frac{4\pi}{10} < j_c > \frac{d}{2}\right)^{\beta+1}\right]^{\frac{1}{\beta+1}} - \frac{2}{d}(H_0 + H_a). \tag{12}$$

We solve eq. (12) self-consistently to find $< j_c >$ and hence other quantities.

For $H_a = 0$, H_1 is always negative, and

$$\frac{4\pi}{10}\langle J_c \rangle_{H=0} = \frac{c}{d} \left[H_0^{\beta+1} + \frac{J_0 H_0^{\beta}(\beta+1)d}{2} \right]^{\frac{1}{\beta+1}} - H_0 \tag{13}$$

3.1. Microscopic field distribution :

Using eq. (7) for H_1 and $H(x) > 0$ and eqs. (9) and (11) for $H_1 < 0$ for generalised power law model, we can get the field distribution $H(x)$ for different value of x for a specified sample

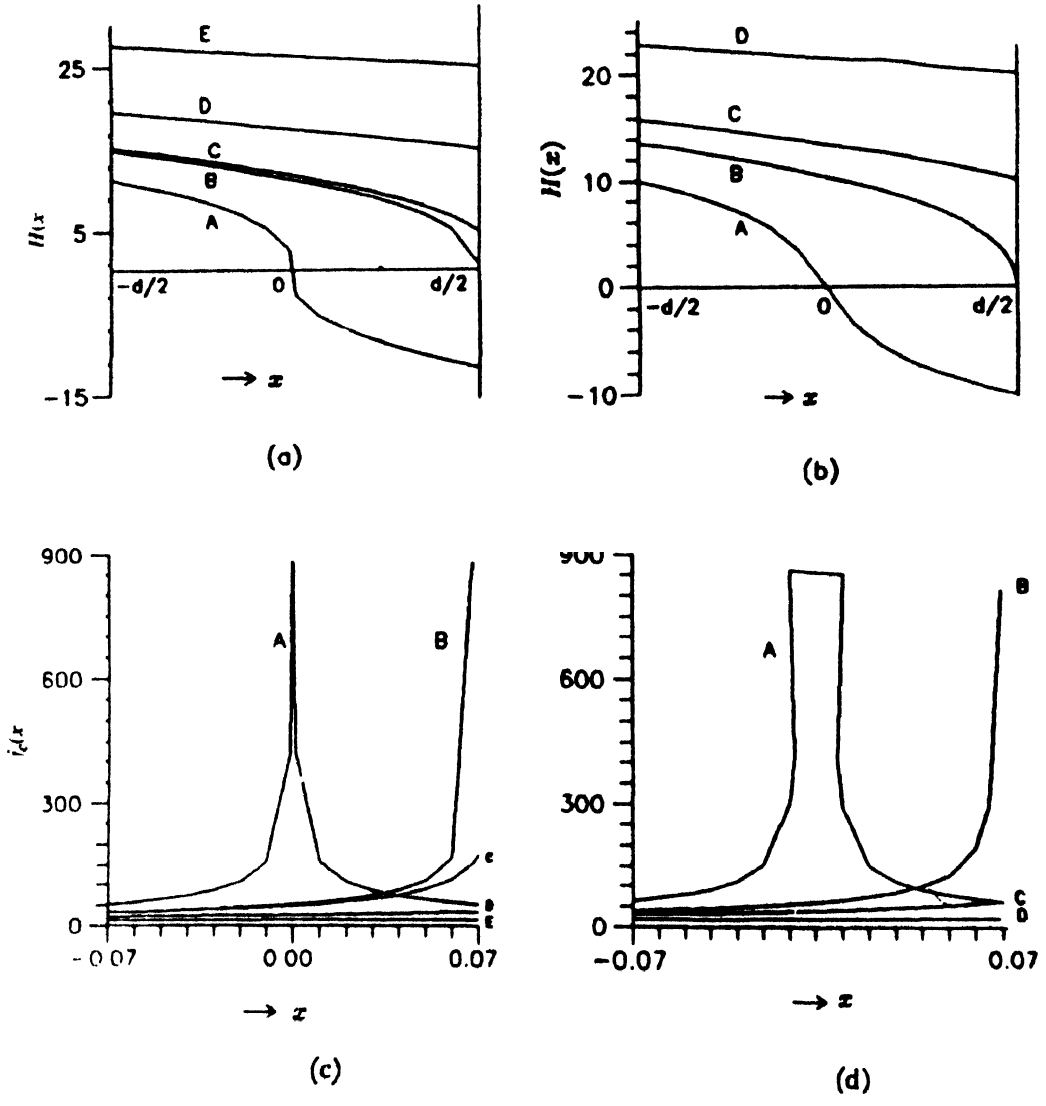

Figure 3. Local field distribution $H(x)$ *vs* x in (a) and (b) and local critical current density $j_c(H(x))$ in (c) and (d) according to generalised and modified power law model respectively.

thickness d. In Figure 3(a), $H(x)$ have been plotted against x. Curve B, C, D, E are for $H_1 > 0$ and A for $H_1 < 0$. The curve B, C, D and E show that for high fields, intergranular field variation reduces and field becomes uniform through out the sample. In Figure 3(b) we have plotted $H(x)$ *vs* x for modified power law model obtained from Ref. [16].

3.2. Local current density distribution :

Once $H(x)$ has been calculated, putting this value in $j_c(H(x))$ gives local average j_c as a function of x. These are plotted for different H_a, in Figure 3(c) for the generalised power law model and in Figure 3(d) for the modified power law model. These graphs show that as H_a is increased j_c becomes progressively more uniform over the cross section of the samples, an observation that was made earlier.

3.3. Bulk critical current density $< j_c >$ *:*

We now compare $< j_c >$ (H) calculated from eqs. (8) and (12) for generalised power law model and from Müller's calculation for modified power low model [16] with our experimental data upto 150 G. To calculate $< j_c >$ from models, we have to estimate the values of H_0 and J_{Co} seperating the value of the product $J_{Co} H_0^{\beta}$ as obtained from high field fitting. It is seen that modified power law model fits our experimental data for three samples with H_0 ~0.3 to 1.2 gauss and generalised power law model fits with H_0 ranging 0.05 to 0.3 gauss [Figure 4(a)]. Since both the models reduce to simple power law relations at higher fields, we should not expect much difference in this region.

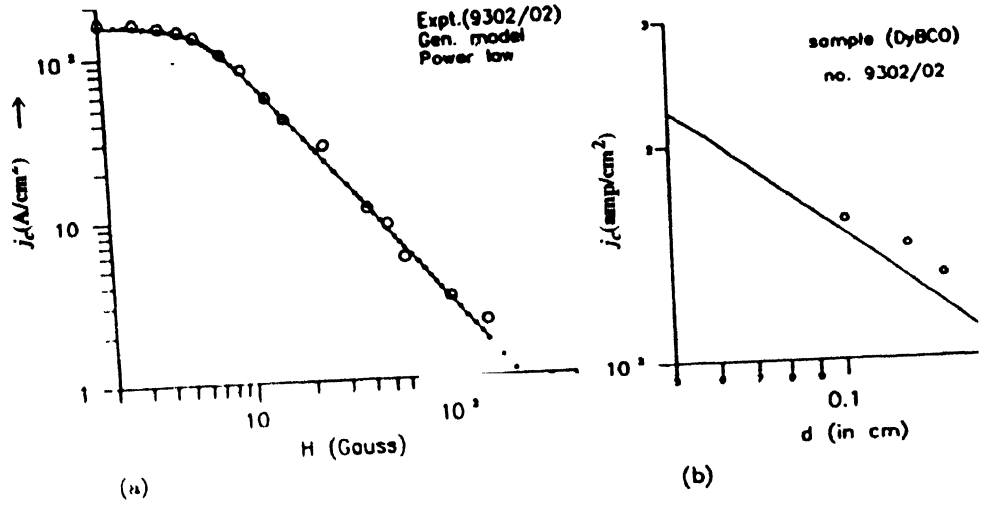

Figure 4. (a) Experimental (o) and calculated (...for GPL model and – for MPL model) values of $< j_c >$ *vs* H upto 150 G; (b) Comparison of experiment and theory for $< j_c >$ $(H_a = 0)$ *vs* d.

If there is any difference, it can show up only at very small fields. In Table 1 we calculated $< j_c >$ for $H_a = 0$ as a function of sample thickness d for both the models (eq. (13) for GPL model) down to d = 10 Å. For both models, $< j_c >$ (0) is found to increase with decreasing d. The calculated values for different d do not differ much. To find out how

Table 1. Change of $< J_c > (H_a = 0)$ with sample thickness d calculated from GPL and MPL models.

Sample thickness	$< J_c > (A/cm^2)$ for $H_a = 0$	
d in cm	GPL	MPL
0.5	60.1	60.5
0.1	150.7	151
0.01	542	554
10^{-3}	1694	1779
10^{-4}	3635	4034
10^{-5}	4512	5416
10^{-6}	4923	5665
10^{-7}	5542	5687

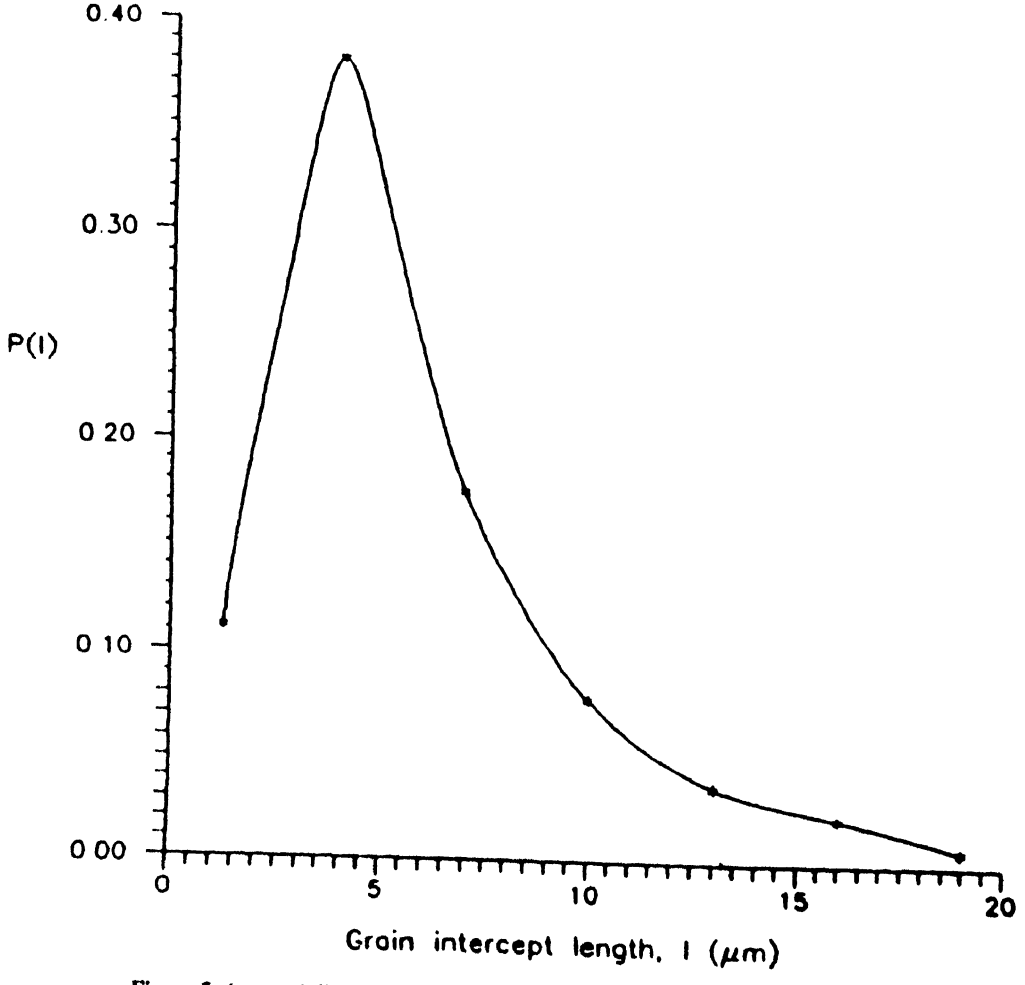

Figure 5. A typical distribution of grain size (from SEM) obtained by length intercept method. Av grain size is 2.46 μm. The skew symmetric nature of the distribution to be noted.

$< j_c > (0)$ depends on slab thickness d, we measured $< j_c >_{H=0}$ for three values of d by successively reducing the thickness for each of the three samples of Dy 123. The experimental results for the sample 9302/02 has been compared with the results calculated with GPL [Figure 4(b)] with the slabs, the thickness cannot be decreased very much due to mechanical constraints. Though Dersch and Blatter [4] went to much smaller cross sections, the configuration used was different from strictly slab geometry. Unless $< j_c > (0)$ is measured for thickness reduced much further (beyond 10^{-3} cm), it will not be possible to decide in favour of one of the two models.

The above analysis shows that the dependence of $< j_c >$ on slab thickness d and the external magnetic field H_a (< 150 G) can be satisfactorily accounted for by the power laws for $j_c(H)$. But $j_c(H)$ is the average current density at a point and is a function of average field at the point. Though this is a local quantity, it is the average over a large number of grains in a granular superconductor. A typical distribution on grain size is shown in Figure 5. Average grain size is 2.46 μm.

4. Hysteresis magnetisation and $< j_c >$

We now calculate hysteresis magnetisation in the frame work of Bean's critical state model. Now

$$\frac{dH(x)}{dx} = \pm \frac{4\pi}{10} j_c\,(H(x)),$$

where the sign depends on the sense of the induced emf. The positive sign corresponds to increasing field and the negative sign to decreasing field. Therefore, the field profile depends on the history of magnetisation.

Field profiles were calculated for

(i) starting from $H_a = 0$ and increasing it to $H_a = H_m$. This gives the virgin part.

(ii) From H_m decreasing to $H_a = 0$, this gives the decreasing part of hysteresis magnetisation.

(iii) Go to $-H_m$ and then increase. On this increasing part, we calculated field profile for $H_a = 0$ to $H_a = H_m$.

The boundary condition is

$$H(d/2) = H_a, \qquad \text{for cylinder}$$

and

$$H(-d/2) = H(d/2) = H_a \qquad \text{for slab.}$$

Then

$$\tilde{B}(H_a) = \frac{\int H dv}{\int dv} \tag{14}$$

and magnetisation M is given by

$$4\pi M(H_a) = -H_a + \tilde{B}(H_a) \tag{15}$$

and

$$\langle j_c \rangle_{H_a} = k\Delta M(H_a) = k(M(H_a\downarrow) - M(H_a\uparrow)). \tag{16}$$

We now calculate the virgin and hysteresis magnetisation cycle using generalised power law model for $j_c(H)$.

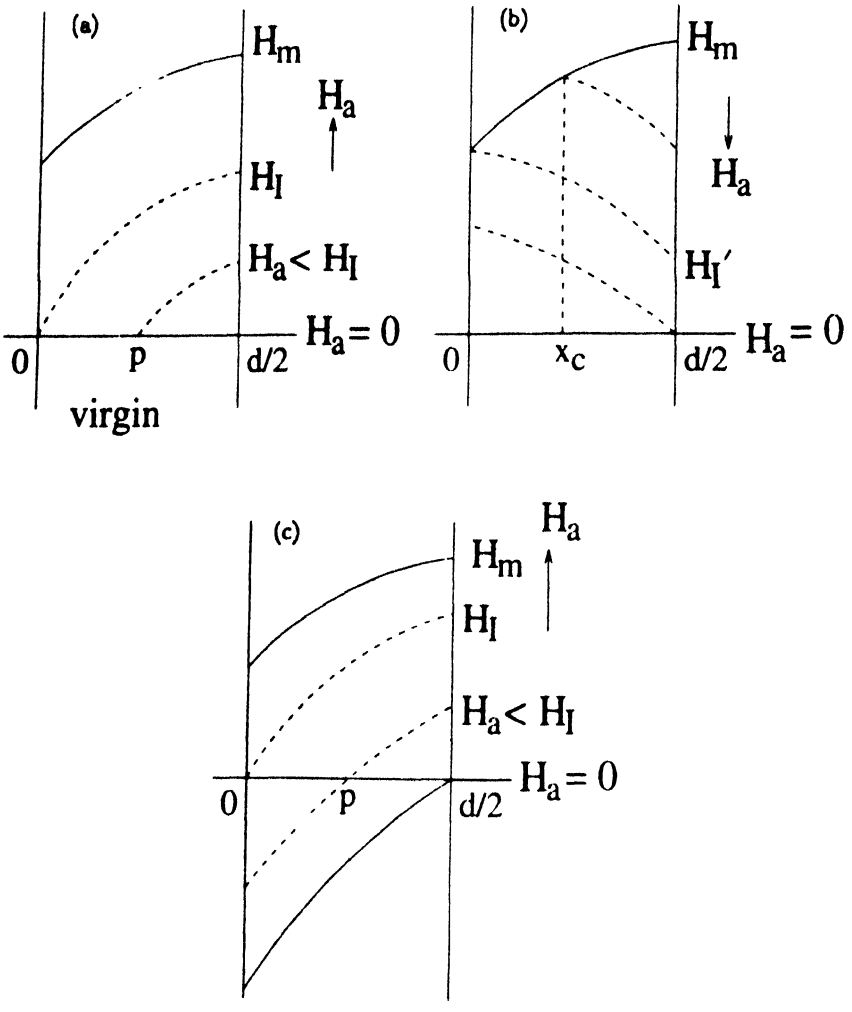

Figure 6. In side field profile $H(x)$ for (a) virgin part; (b) decreasing H_a starting from H_m in a hysteresis cycle; (c) increasing H_a starting from $-H_m$ in a hysteresis cycle.

4.1. Virgin magnetisation :

In this part, H_I is an external applied magnetic field for which $H(0) = 0$ [Figure 6(a)]. Substituting

$$q = \left|1 + \frac{H_a}{H_0}\right|^{\beta+1}$$

$$r = \frac{J_0 d(\beta+1)}{2H_0},$$

$$b_0 = \frac{1}{2}(q + q_m),$$

$$p = \frac{d}{2}\frac{(r+1-q)}{r},$$

$$\alpha = \frac{1}{\beta+1},$$

$$x_c = \frac{d}{2}\left(1 - \frac{q_m - q}{2r}\right)$$

and using relation (14), we get expression for $B(H_a)$.

For $H_a < H_l$,

$$\tilde{B}(H_a)_{\text{slab}} = \frac{H_0}{r(\alpha+1)}\left(q^{\alpha+1} - 1\right) - H_0(1 - 2p/d), \tag{17}$$

$$\tilde{B}(H_a)_{\text{cylin}} = \frac{8H_0}{d^2}\left[\frac{d}{2r(\alpha+1)}\left(\frac{d}{2}q^{\alpha+1} - p\right)\right.$$

$$\left. - \left(\frac{d}{2r}\right)^2 \frac{1}{(\alpha+1)(\alpha+2)}\left(q^{\alpha+2} - 1\right) - \frac{1}{2}\left\{(d/2)^2 - p^2\right\}\right] \tag{18}$$

and for $H_a > H_l$,

$$\tilde{B}(H_a)_{\text{slab}} = \frac{H_0}{r(\alpha+1)}\left[q^{\alpha+1} - (q-r)^{\alpha+1}\right] - H_0, \tag{19}$$

$$\tilde{B}(H_a)_{\text{cylin}} = \frac{8H_0}{d^2}\left[\frac{d^2}{4r(\alpha+1)}q^{\alpha+1} - \left(\frac{d}{2r}\right)^2 \frac{1}{(\alpha+1)(\alpha+2)}\right.$$

$$\left. \times\left\{q^{\alpha+2} - (q-r)^{\alpha+2}\right\} - d^2/8\right] \tag{20}$$

4.2. Hysteresis magnetisation :

(i) decreasing part of hysteresis cycle from $H_a = H_m$ to 0 :

In this part [see Figure 6(b)] for $H_a > H_l$,

$$\tilde{B}(H_a)_{\text{slab}} = \frac{H_0}{r(\alpha+1)}\left[2b_0^{\alpha+1} - q^{\alpha+1} - (q_m - r)^{\alpha+1}\right] - H_0, \tag{21}$$

$$\tilde{B}(H_a)_{\text{cylin}} = \frac{8H_0}{d^2}\left[\frac{d}{2r(\alpha+1)}\left\{2x_c b_0^{\alpha+1} - q^{\alpha+1}\frac{d}{2}\right\}\right.$$

$$\left. - \left(\frac{d}{2r}\right)^2 \frac{1}{(\alpha+1)(\alpha+2)}\left\{q^{\alpha+2} - (q_m - r)^{\alpha+2}\right\} - \frac{d^2}{8}\right] \tag{22}$$

and for $H_a < H_l$,

$$\tilde{B}(H_a)_{\text{slab}} = \frac{H_0}{r(\alpha+1)}\left[(q+r)^{\alpha+1} - q^{\alpha+1}\right] - H_0, \tag{23}$$

$$\tilde{B}(H_a)_{\text{cylin}} = \frac{8H_0}{d^2}\left[-\frac{d^2}{4r(\alpha+1)}q^{\alpha+1} + \left(\frac{d}{2r}\right)^2 \times \frac{1}{(\alpha+1)(\alpha+2)}\left\{(q+r)^{\alpha+2} - q^{\alpha+2}\right\} - \frac{d^2}{8}\right]. \tag{24}$$

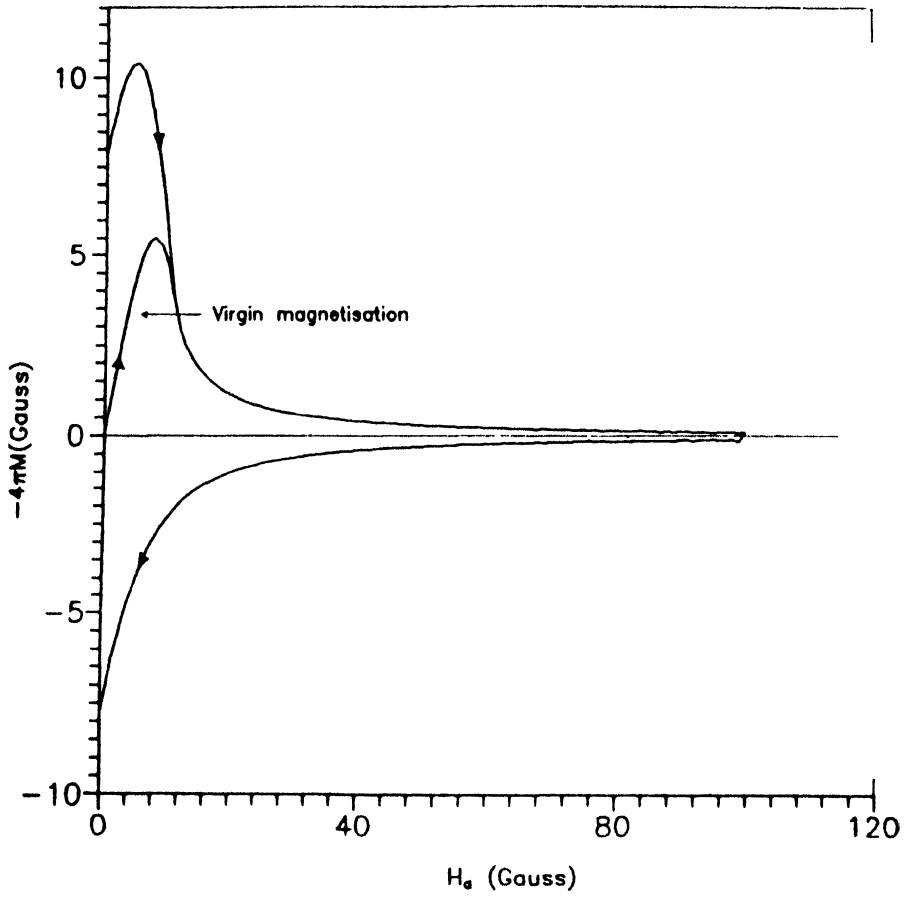

Figure 7. Plot of $-4\pi M$ vs H_a

(ii) increasing part of hysteresis cycle from $H_a = 0$ to H_m:

In this part [see Figure 6(c)] for $H_a < H_1$,

$$\tilde{B}(H_a)_{\text{slab}} = \frac{H_0}{r(\alpha+1)}\left\{q^{\alpha+1} - (1 + 2rp/d)^{\alpha+1}\right\} + H_0(4p/d - 1), \tag{25}$$

$$\tilde{B}(H_a)_{\text{cylin}} = \frac{8H_0}{d^2}\left[\frac{d^2}{4r(\alpha+1)}q^{\alpha+1} - \left(\frac{d}{2r}\right)^2 \frac{1}{(\alpha+1)(\alpha+2)} \times \left\{q^{\alpha+2} + \left(1 + \frac{2rp}{d}\right)^{\alpha+2} - 2\right\} + p^2 - \frac{d^2}{8}\right] \tag{26}$$

and for $H_a > H_l$, expressions for $\tilde{B}(H_a)$ will be same as eqs. (19) and (20) for slab and cylinder respectively.

5. Results of calculation

As we have measured critical current density $< j_c >$ for a slab geometry, we shall here show the results of calculation of hysteresis magnetisation and $< j_c >$ for slab of thickness d using the same value of β and H_0 that we have used in Section 3. Figure 7 shows the results of hysteresis magnetisation obtained using relation (15) with the applied magnetic field, H_a.

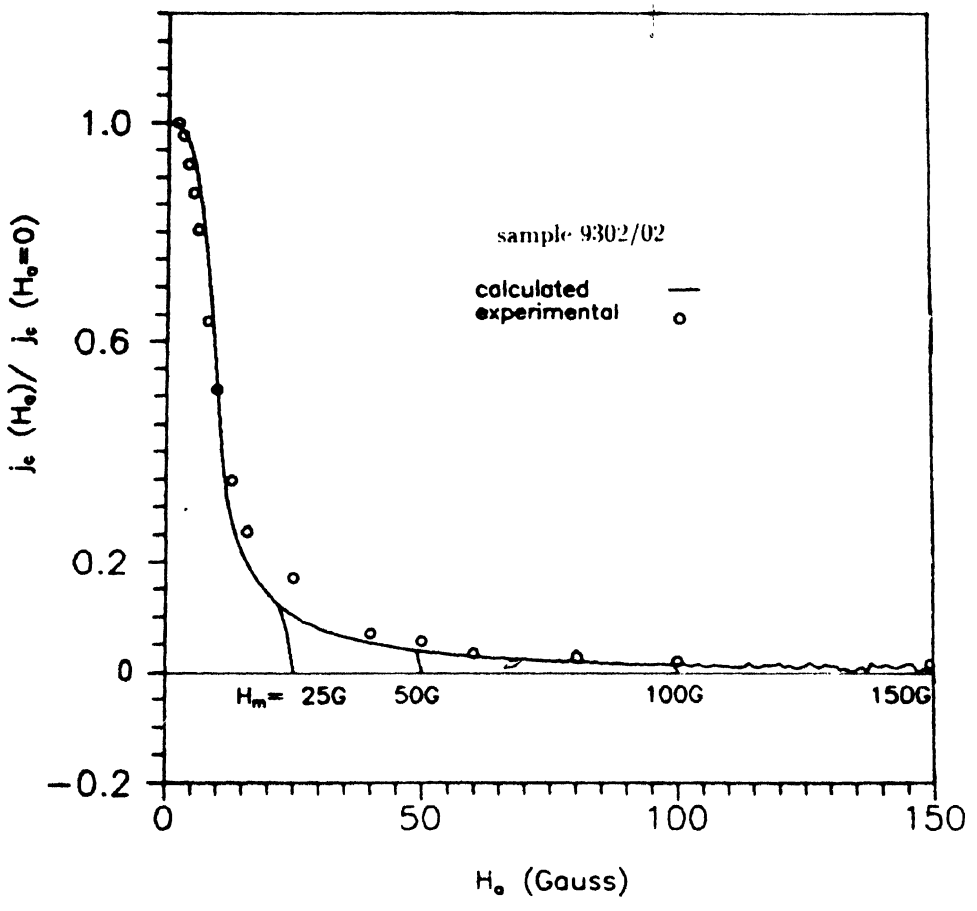

Figure 8. Comparison of $< j_c >_{H_a} / < j_c >_{H_a=0}$ obtained from experiment and hysteresis magnetisation calculation of generalised power law model.

Calculating $\Delta M(H_a)$ between $M(H_a \downarrow)$ and $M(H_a \uparrow)$ for a given H_a and then applying relation (16), we obtained $< j_c >$. In Figure 8, a comparison of $< j_c >_{H_a} / < j_c >_{H_a=0}$ obtained from experiment and hysteresis magnetisation calculation has been shown. Figure 8 shows that critical current density obtained from hysteresis magnetisation using generalised power law model fit experimental data extremely satisfactorily.

6. Conclusions

The power law exponent $\beta = 1.5$ is consistent with currents limited by Josephson weak links at the grain boundaries proposed by Peterson and Ekin [5]. Thus upto about 150 G (low field), the intragrain effects have not come into play. In the low field region, experimentally obtained variation of critical current density with applied magnetic field can be satisfactorily accounted for by the generalised power law model both from transport current and hysteresis magnetisation calculation in the frame work of Bean's critical state model with the same value of β and H_0. The generalised power law model is more appealing since various critical state models (Kim, Bean's original, Power law, Exponential) follow from it under specific conditions.

Acknowledgment

We thank the University Grants Commission for financial assistance to carry out the work. First author also thank the Council of Scientific & Industrial Research for providing his scholarship to continue the research work on the subject.

References

[1] C P Bean *Phys. Rev. Lett.* **8** 250 (1962); *Rev. Mod. Phys.* **36** 31 (1964)

[2] A A Abrikosov *Sov. Phys. JETP* **5** 1174 (1957)

[3] P W Anderson and Y B Kim *Rev. Mod. Phys.* **36** 39 (1964)

[4] H Dersch and G Blatter *Phys. Rev.* **B38** 11391 (1988)

[5] R L Peterson and J W Ekin *Physica* **C157** 325 (1989)

[6] K-H Müller, D N Matthews, R Driver and C Andrikidis *Cryogenics* **32** 256 (1992) *ICMC Supplement*

[7] D N Matthews and K-H Müller *J. Appl. Phys.* **72**(7) 2964 (1992)

[8] K-H Müller and D N Matthews *IEEE Transactions on Applied Superconductivity* **3** 1229 (1993)

[9] *Proceedings of the 7th International Workshop on Critical Currents in Superconductors* ed. H W Weber (Singapore : World Scientific) (1994)

[10] G Ravi Kumar *PhD Thesis* (Bombay University, India) (1990)

[11] G Ravi Kumar and P Chaddah *Phys. Rev.* **B39** 4704 (1989)

[12] Y Yeshurun, M W McElfresh, A P Malozemoff, J Hagerh horst-Trewhella, J Mannhart, F Holtzberg and G V Chandrashekhar *Phys. Rev.* **B42** 6322 (1990)

[13] Donglu Shi, M Xu, A Umezawa and R F Fox *Phys. Rev.* **B42** 2062 (1990)

[14] A Sanchez, D-X Chen, J S Munoz and Y-Z Li *Physica* **C175** 33 (1991)

[15] S Sengupta and D Shi *High Temperature Superconducting Materials Science and Engineering* ed. Donglu Shi (Oxford : Pergamon) p 139 (1993)

[16] K-H Müller, D N Matthews and R Driver *Physica* **C191** 339 (1992)